Epitaxial Growth of LaB_6 Thin Films on Ultrasmooth Sapphire Substrate with Epitaxial SrB_6 Buffer Layer

Yushi KATO[*1], Naoki SHIRAISHI[*1], Satoru KANEKO[*2], Nobuo TSUCHIMINE[*3], Susumu KOBAYASHI[*3] and Mamoru YOSHIMOTO[*1, *4]

[*1] *Department of Innovative & Engineered Materials, Tokyo Institute of Technology, 4259-J2-46, Nagatsuta-cho, Midori-ku, Yokohama 226-8503, Japan*
E-mail:kato.y.am@m.titech.ac.jp
[*2] *Kanagawa Industrial Technology Research Institute, 705-1 Shimo-Imaizumi, Ebina, Kanagawa 243-0435, Japan*
[*3] *TOSHIMA Manufacturing Company Limited, 1414, Shimonomoto, Higashimatsuyama-shi, Saitama 355-0036, Japan*
[*4] *Patent Attorney, Tokyo Institute of Technology, 4259-J2-46, Nagatsuta-cho, Midori-ku, Yokohama 226-8503, Japan*

We fabricated epitaxial LaB_6 (100) thin films on ultrasmooth sapphire (α-Al_2O_3 single crystal) (0001) substrate with epitaxial SrB_6 buffer layer by laser molecular beam epitaxy. Reflection high-energy electron diffraction and X-ray diffraction measurements indicate the heteroepitaxial structure of LaB_6 (100)/SrB_6 (100)/sapphire (0001) with three domains of epitaxial relationship. The prepared films exhibit atomically stepwise surface morphology, similar to that for the substrate, with 0.2-nm-high atomic steps and ~70-nm-wide terraces. LaB_6 epitaxial thin films show metallic behavior, with almost constant resistivity (1.0×10^{-3} Ω cm) in the temperature range 10–300 K, while epitaxial SrB_6 buffer thin films show semiconducting behavior, with a resistivity of 4.8 Ω cm at room temperature.

DOI: 10.2961/jlmn.2009.03.0010

Keywords: hexaboride, LaB_6, SrB_6, laser MBE, epitaxial thin film, electrical properties

1. Introduction

Alkaline hexaborides, such as SrB_6, CaB_6, and BaB_6, and rare earth hexaborides, such as LaB_6, EuB_6, and CeB_6, have attractive physical properties. Their structure is a CsCl-type simple cubic arrangement composed of B_6 octahedra and metal ions [1-4]. Interestingly, their electrical properties vary widely, from semiconducting [5] to superconducting [6], upon doping divalent or trivalent metallic ions into the crystal structure.

LaB_6 has a high melting temperature, excellent thermal stability, high hardness, and excellent chemical stability [1-4,7-9]. It is often used in thermionic electron sources for transmission electron microscopy, scanning electron microscopy, and flat panel displays, for which it offers high brightness and long service life because of its extremely small work function (~2.4 eV), high current and voltage capability, and low vapor pressure at high temperature. Its electric conduction reportedly shows metallic properties [1,7,8].

Investigations into the properties of LaB_6 have been conducted mostly on bulk samples [1-4,7-9]. The properties of LaB_6 thin films have not been well explored. There have been a few attempts to prepare LaB_6 nanowire by chemical vapor deposition [10] and LaB_6 polycrystalline thin films by sputtering [11,12], e-beam evaporation [13], and pulsed laser deposition (PLD) [14-17]. However, there are few reports on fabrication of epitaxial LaB_6 thin films [18], although heteroepitaxial growth of hexaboride thin films is of great interest for their applicability in thermoelectric conversion materials [19] and high-performance electronic devices.

We previously investigated low-temperature epitaxial growth of functional ceramic thin films of oxides [20-22], nitrides [23,24], and diamond [25] by PLD or laser molecular beam epitaxy (MBE) (that is, pulsed laser deposition in ultrahigh vacuum) on ultrasmooth sapphire (α-Al_2O_3 single crystal) (0001) substrate. The smooth substrate has 0.2-nm-high atomic steps and 60–80-nm-wide atomically flat terraces [26]. Laser MBE has been used extensively to grow epitaxial thin films of high-melting-point ceramics at relatively low substrate temperatures [20-25].

Recently, we fabricated highly (100)-oriented LaB_6 polycrystalline thin films and epitaxial SrB_6 thin films on the ultrasmooth sapphire (0001) substrate by laser MBE [17]. In this study, we grew epitaxial LaB_6 thin films on ultrasmooth sapphire (0001) substrate with epitaxial SrB_6 buffer layer by laser MBE and characterized the film's morphological, crystallographic, and electrical properties.

2. Experimental details

Fabrication of SrB_6 and LaB_6 thin films was carried out by laser MBE (~10^{-7} Pa base pressure) on ultrasmooth sapphire (0001) substrate. The substrate was obtained by annealing commercially available mirror-polished α-Al_2O_3 single crystal wafers at 1000 °C for 3 h in air [26]. The step height was uniformly ~0.2 nm, and the terrace width was 60–80 nm. A pulsed KrF excimer laser (248 nm wavelength, 20 ns pulse duration, 0.5 mm^2 beam spot size) was

focused on a sintered ceramic target of SrB_6 and LaB_6 (both 99.5% purity), with energy densities of 1.5 and 3.0 J/cm^2 and frequencies of 3 and 5 Hz, respectively. The distance between the substrate and the target was 5 cm. The ablated particles collided with the substrate heated at 800 °C to form the films. The elapsed time of deposition for SrB_6 and LaB_6 was 30 and 60 min, respectively.

Crystallinity and surface atomic structure during film deposition were characterized by in situ reflection high-energy electron diffraction (RHEED). Crystallographic structure was characterized by ex situ X-ray diffraction (XRD; MXP-M18, Bruker AXS) using CuKα line (λ = 0.1542 nm). The film surface morphology was observed in air by atomic force microscopy (AFM; SPI-3700, Seiko Instruments). The film surface work function φ was determined using a Kelvin probe (KP) in air. The film resistivity was measured by the conventional four-probe method in the temperature range 10–300 K.

3. Results and discussion

First, we examined the epitaxial growth of LaB_6 films deposited directly on sapphire substrate. Fig. 1 shows the XRD pattern and RHEED image for a LaB_6 thin film (30 nm) on sapphire substrate without epitaxial SrB_6 buffer layer. From the XRD pattern and the ring RHEED image, LaB_6 thin film was not epitaxial, but the (100) highly oriented polycrystalline film with the in-plane random configuration. We found that the lattice mismatch (12.7%) between sapphire and LaB_6 is very large to carry out successful epitaxial growth of LaB_6 films on sapphire (0001) substrate.

Next, we considered the possibilities of SrB_6 buffer layer to reduce lattice mismatch between LaB_6 and sapphire (0001), because the lattice mismatch between LaB_6 and SrB_6 is just 0.9%. Fig. 2 shows the XRD pattern and RHEED image for a SrB_6 thin film (15 nm) on sapphire substrate. The streaky RHEED image and evident in-plane anisotropy indicate epitaxial film growth. From the XRD pattern, SrB_6 (100) and (300) peaks are observed, and the SrB_6 (200) peak overlaps with the sapphire (0006) peak. The root-mean-square (RMS) roughness of the film on the substrate is 0.10 nm. The film exhibits atomically stepwise surface morphology, similar to that for the substrate, with 0.2-nm-high atomic steps and ~70-nm-wide terraces. Thus, epitaxial SrB_6 (100) thin films can be fabricated on ultrasmooth sapphire substrate and are suitable for use as a buffer layer.

To determine the influence of an ultrathin epitaxial SrB_6 buffer layer, we grew LaB_6 thin films on ultrasmooth sapphire substrate, with and without epitaxial SrB_6 buffer layer, under the same conditions. Fig. 3 shows the XRD pattern and RHEED image for a LaB_6 thin film (30 nm) on sapphire substrate with epitaxial SrB_6 buffer layer (5 nm). The RHEED image is streaky, and the image intensity and pattern change with incident beam direction. The streaky image and evident in-plane anisotropy indicate epitaxial film growth. From the XRD pattern, LaB_6 (100) and (200) planes are observed. Although slight reflection peak of LaB_6 (111) was observed, it was found that LaB_6 thin films with single phase were grown preferentially compared to the growth without SrB_6 buffer, as shown in insets of the Fig. 3. Thus, epitaxial LaB_6 (100) thin films can be fabricated on ultrasmooth sapphire substrate with epitaxial SrB_6 buffer layer, and the buffer layer promotes epitaxial growth of the films.

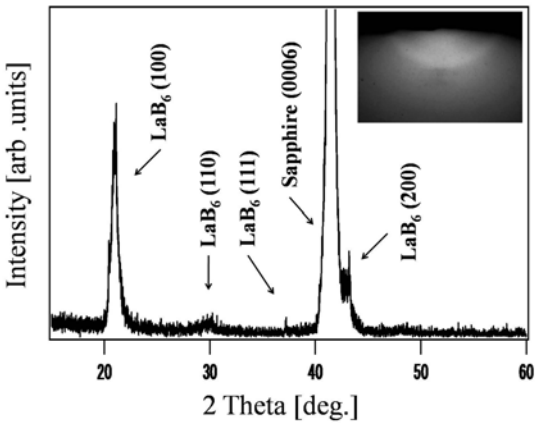

Fig. 1 XRD pattern of LaB_6 thin film on sapphire substrate without SrB_6 buffer layer. Inset: RHEED image viewed along the sapphire [10-10] axis.

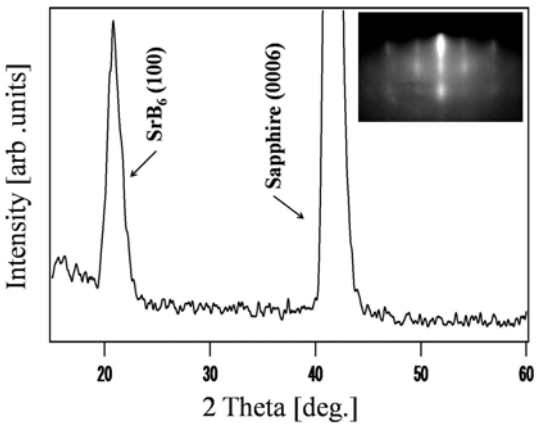

Fig. 2 XRD pattern of SrB_6 thin film on sapphire substrate. Inset: RHEED image viewed along the sapphire [10-10] axis.

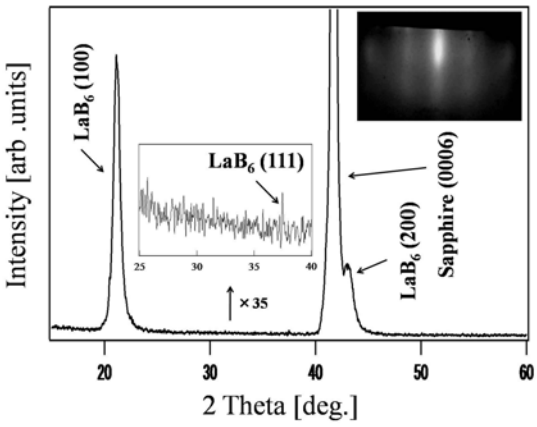

Fig. 3 XRD pattern of LaB_6 thin film on sapphire substrate with SrB_6 buffer layer. Insets: magnified (×35) view of XRD pattern in the 2 theta range 25-40 deg. and RHEED image viewed along the sapphire [10-10] axis.

We investigated the crystal structure and in-plane orientation of the obtained LaB_6 epitaxial thin film by rotary φ-scan XRD using a four-circle X-ray diffractometer. Fig. 4 shows the azimuthal φ-scan XRD result for LaB_6 (101) peaks. Peaks (circle, triangle, square) are observed at every 60° phi rotation. Small peaks (dotted circle, dotted triangle, dotted square) are similarly observed. For a simple cubic LaB_6/SrB_6 layer grown on sapphire substrate, the small peaks will be more clearer, indicating that the LaB_6 thin film and SrB_6 buffer layer grow as a tetragonal-like cubic, not simple cubic, structure since the in-plane lattice misfit over the two materials (SrB_6 and sapphire) is −11.9 and 1.8% in the [1-100] and [11-20] directions, respectively, of sapphire.

Thus, three domains of LaB_6/SrB_6 layer on sapphire substrate were grown with in-plane two-folded symmetry. The critical thickness between SrB_6 and sapphire was estimated theoretically by the People–Bean formula [27]

$$h_c \approx (\frac{1-\nu}{1+\nu})(\frac{1}{16\pi\sqrt{2}})(\frac{b^2}{a_{epi}})[(\frac{1}{f^2})\ln(\frac{h_c}{b})], \quad (1)$$

where h_c is the critical thickness, ν is the Poisson ratio, b is the slip distance, a_{epi} is the lattice constant for the SrB_6 epitaxial layer, and f is the lattice mismatch between SrB_6 and sapphire. The critical thickness (~40 nm) in the [11-20] direction of sapphire can be calculated, while that in the [1-100] direction cannot since the misfit is too large. This implies that strain relaxation begins immediately after film deposition in the [1-100] direction of sapphire; in contrast, it will not begins until 40 nm film thickness in the [11-20] direction of sapphire [28]. In fact, the crystalline films of the LaB_6/SrB_6/sapphire and SrB_6/sapphire systems turn from epitaxial to polycrystalline with increasing film thickness. XRD and RHEED measurements indicate the heteroepitaxial structure of LaB_6 (100)/SrB_6 (100)/sapphire (0001) with three domains of epitaxial relationship: LaB_6 [001]//SrB_6 [001]//sapphire [1-100], LaB_6 [001]//SrB_6 [001]//sapphire [10-10], and LaB_6 [001]//SrB_6 [001]//sapphire [01-10].

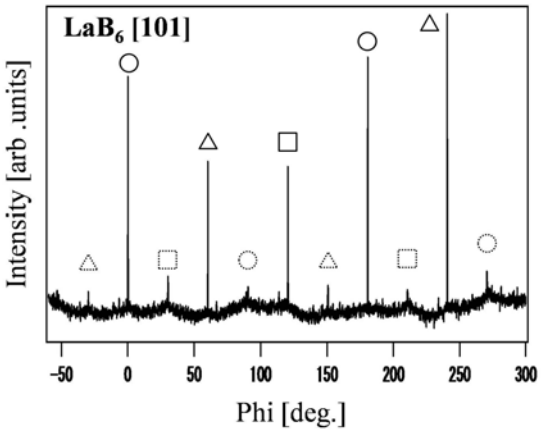

Fig. 4 φ–scan XRD pattern of LaB_6 thin film on sapphire (0001) substrate with SrB_6 (100) buffer layer.

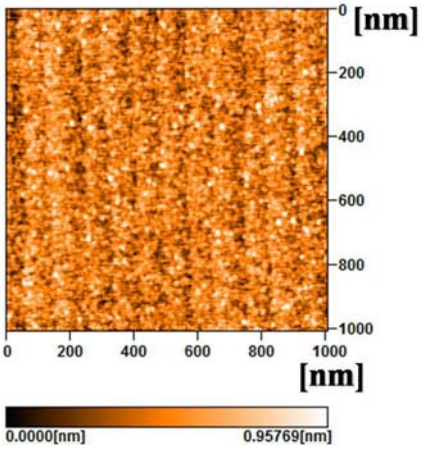

Fig. 5 AFM surface image of LaB_6 thin film on sapphire substrate with SrB_6 buffer layer.

Fig. 5 shows the AFM surface image of the prepared LaB_6 thin film on sapphire substrate with epitaxial SrB_6 buffer layer. The average diameter of the observed grain-like islands agrees well with that calculated by Sherrer's equation (~20 nm). The film surface is atomically flat (RMS roughness 0.28 nm) and exhibits straight atomic steps derived from the surface of the substrate.

From the earliest considerations of the electronic structure of metal hexaborides, it has been predicted that those formed from trivalent metals would be metallic electrical conductors and those formed from divalent metals would be semiconductors [7,29]. Fig. 6 shows the temperature dependence of resistivity for a SrB_6 thin film on sapphire substrate; the inset shows a magnified view of the curve in the temperature range 250–300 K. The film shows semiconducting behavior, and the resistivity is about 5 Ω cm at room temperature. Two different regions of activated behavior can be identified [5]. Low-temperature and high-temperature regions were fit independently to an activated form by the Arrhenius equation

$$\rho(T) = \rho_0 \exp(\Delta E / k_B T), \quad (2)$$

where ΔE is the activation energy, ρ_0 is the resistivity at large temperature T. The fit results are in excellent agreement with a semiconducting model in which the high-temperature fit gives a gap of ~38.2 meV and the low-temperature fit gives a much smaller gap of ~0.5 meV. These gaps are about 10 times larger than for a single-crystal bulk sample (5.8 meV in the high-temperature range and 0.09 meV in the low-temperature range) [5].

Fig. 7 shows the temperature dependence of resistivity for a LaB_6 thin film on sapphire substrate with epitaxial SrB_6 buffer layer. The film shows metallic behavior, and the resistivity is almost constant (1.0×10^{-3} Ω cm) in the temperature range 10–300 K. The room-temperature resistivities for the epitaxial LaB_6 and SrB_6 films are about 100 times larger than those reported for single-crystal bulk LaB_6 and SrB_6 [1,5].

In general, the difference in resistivity for bulk crystal and thin film is considered to be caused by various effects of impurity, deficiency, internal stress, and compositional

nonstoichiometry that exist in thin films. For alkaline earth hexaborides such as SrB_6, the valence-band maximum and conduction-band minimum are sensitive to the intra B-octahedron bond length; therefore, the band gap depends on the lattice parameter [30]. Thus, considering that the lattice parameter of the films (a_0 = 0.4255 nm) is larger than that of bulk SrB_6 (a_0 = 0.4195 nm), resistivity is affected by the lattice parameter.

On the other hand, from the band calculation for LaB_6, the Fermi surface consists of strongly hybridized orbitals formed by hybridization between boron *sp* orbitals and lanthanum *d* orbitals, so boron vacancies can seriously disturb electron conduction paths [13]. To determine the influence of electron conduction paths, we calculated the mean free path of an electron carrier in our sample and compared it with that for the bulk sample reported previously [8,13]. The mean free path l of an electron carrier in our sample was estimated by Matthiessen's rule [13]

$$l = (r.r.r. - 1)[\rho l]_{Bulk} / \rho_{(T=300K)}, \quad (3)$$

where $[\rho l]_{Bulk}$ is the bulk value of ρl (2.1×10^{-11} Ω cm^2 for LaB_6 [8]), *r.r.r.* is the residual resistance ratio, and $\rho_{(T = 300\ K)}$ is the bulk resistivity at 300 K (8.9×10^{-6} Ω cm for LaB_6). Thus, the mean free path l for the film is about 0.8 nm, much smaller than that for the bulk material (~6.98 μm [8,13]). Since the grain size d (~20 nm) from the XRD and AFM results is larger than the mean free path l estimated for this sample, the effect of grain-boundary scattering on electron conduction is considered to be smaller than the effect of inter-grain scattering, including electron–electron, electron–phonon, and impurity/defect scattering. The relationship between electrical properties and composition in the thin film system is not clear at present and requires further investigation.

When examining LaB_6 thin films with a view toward their application as cathode materials and electronic devices, an important property is the work function φ. For reference, we measured φ for gold thin film, which is known to be good standard [31,32] and whose value we assumed to be 5.28 eV. From KP results, we estimated φ for bulk LaB_6 and LaB_6 thin film to be 4.53 and 4.54 eV, respectively.

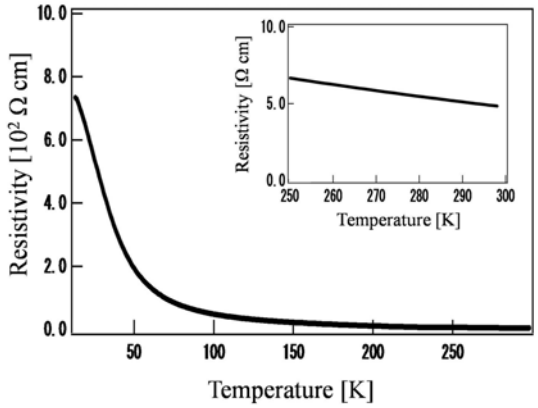

Fig. 6 Temperature dependence of resistivity for SrB_6 thin film on sapphire substrate. Inset: magnified view in the temperature range 250–300 K.

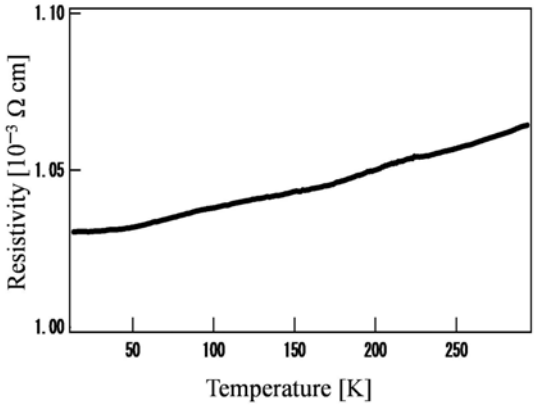

Fig. 7 Temperature dependence of resistivity for LaB_6 thin film on sapphire substrate with SrB_6 buffer layer.

These values do not agree with the previous reported value for the (001) clean surface of single-crystal bulk LaB_6 (2.4–2.6 eV) [2,3]. Since our measurements were performed in air, the surface of the sample should be covered with adsorbates such as oxygen and hydrogen, which may affect measurement. Further studies are thus necessary to determine the surface properties of hexaboride thin films.

4. Conclusions

We fabricated epitaxial LaB_6 (100) thin films on ultrasmooth sapphire (α-Al_2O_3 single crystal) (0001) substrate with epitaxial SrB_6 buffer layer. RHEED and XRD measurements indicate the heteroepitaxial structure of LaB_6 (100)/SrB_6 (100)/sapphire (0001) with three domains of epitaxial relationship: LaB_6 [001]//SrB_6 [001]//sapphire [1-100], LaB_6 [001]//SrB_6 [001]//sapphire [10-10], and LaB_6 [001]//SrB_6 [001]//sapphire [01-10]. The films exhibit atomically stepwise surface morphology, similar to that of the substrate, with 0.2-nm-high atomic steps and ~70-nm-wide terraces. They are epitaxial in nature and show metallic behavior, with almost constant resistivity (1.0×10^{-3} Ω cm) in the temperature range 10–300 K. In contrast, the epitaxial SrB_6 thin films show semiconducting behavior, with a resistivity of 4.8 Ω cm at room temperature.

Acknowledgments

This work was supported in part by the Ministry of Education, Culture, Sports, Science and Technology of Japan, the National Institute of Advanced Industrial Science and Technology of Japan, the New Energy and Industrial Technology Development Organization of Japan, and the Regional Innovation Creation R&D Program of the Ministry of Economy, Trade and Industry of Japan.

References

[1] D. Mandrus, B. C. Sales and R. Jin: Phys. Rev. B, 64, (2001) 012302.
[2] M. Aono, R. Nishitani, C. Oshima, T. Tanaka, E. Bannai and S. Kawai: J. Appl. Phys., 50, (1979) 4802.
[3] M. Aono, C. Oshima, T. Tanaka, E. Bannai and S. Kawai: J. Appl. Phys., 49, (1978) 2761.
[4] C. -H. Chen, T. Aizawa, N. Iyi, A. Sato and S. Otani: Journal of Alloys and Compounds, 366, (2004) L6.

[5] H. R. Ott, M. Chernikov, E. Felder, L. Degiorgi, E. G. Moshopoulou, J. L. Sarrao and Z. Fisk: Z. Phys. B, 102, (1997) 337.
[6] R. J. Sobczak and M. J. Sienko: J. Less-Com. Metals, 67, (1979) 167.
[7] A. Hasegawa and A. Yanase: J. Phys. F: Metal Phys., 7, (1977) 1245.
[8] T. Tanaka, T. Akahane, E. Bannai, S. Kawai, N. Tsuda and Y. Ishizawa: J. Phys. C: Solid State Phys., 9, (1976) 1235.
[9] M. Zhang, L. Yuan, X. Wang, H. Fan, X. Wang, X. Wu, H. Wang and Y. Qian: J. Solid State Chem., 181, (2008) 294.
[10] H. Zhang, Q. Zhang, J. Tang and L. -C. Qin: J. Am. Chem. Soc., 127, (2005) 2862.
[11] C. Mitterer: J. Solid State Chem., 133, (1997) 279.
[12] T. Nakano, S. Baba, A. Kobayashi, A. Kinbara, T. Kajiwara and K. Watanabe: J. Vac. Sci. Technol. A, 9, (1991) 547.
[13] I. Terasaki, S. Uchida, S. Tajima, K. Uchinokura and S. Tanaka: J. Phys. Soc. Jpn., 59, (1990) 1017.
[14] V. Craciun and D. Craciun: Appl. Surf. Sci., 247, (2005) 384.
[15] D. J. Late, K. S. Date, M. A. More, P. Misra, B. N. Singh, L. M. Kukreja, C. V. Dharmadhikari and D. S. Joag: Nanotechnology, 19, (2008) 265605.
[16] D. J. Late, M. A. More, P. Misra, B. N. Singh, L. M. Kukreja and D. S. Joag: Ultramicroscopy, 107, (2007) 825.
[17] Y. Kato, Y. Ono, Y. Akita, M. Hosaka, N. Shiraishi, N. Tsuchimine, S. Kobayashi and M. Yoshimoto: Mat. Res. Soc. Symp. Proc., 1148, (2009) PP12-02.
[18] S. Muranaka and S. Kawai: J. Appl. Phys. Jpn., 15, (1976) 587.
[19] M. Takeda, T. Fukuda, F. Domingo and T. Miura: J. Solid State Chem., 177, (2004) 471.
[20] J. Tashiro, A. Sasaki, S. Akiba, S. Satoh, T. Watanabe, H. Funakubo and M. Yoshimoto: Thin Solid Films, 415, (2002) 272.
[21] T. Maeda, M. Yoshimoto, T. Ohnishi, G. H. Lee and H. Koinuma: J. Cryst. Growth, 177, (1997) 95.
[22] A. Sasaki, W. Hara, A. Matsuda, N. Tateda, S. Otaka, S. Akiba, K. Saito, T. Yodo and M. Yoshimoto: Appl. Phys. Lett., 86, (2005) 231911.
[23] W. Hara, J. Liu, A. Sasaki, S. Otaka, N. Tateda, K. Saito and M. Yoshimoto: Thin Solid Films, 516, (2008) 2889.
[24] A. Sasaki, J. Liu, W. Hara, S. Akiba, K. Saito, T. Yodo and M. Yoshimoto: J. Mater. Res., 19, (2004) 2725.
[25] M. Yoshimoto, K. Yoshida, H. Maruta, Y. Hishitani, H. Koinuma, S. Nishio, M. Kakihana and T. Tachibana: Nature, 399, (1999) 340.
[26] M. Yoshimoto, T. Maeda, T. Ohnishi, O. Ishiyama, M. Shinohara, M. Kubo, R. Miura, A. Miyamoto and H. Koinuma: Appl. Phys. Lett., 67, (1995) 2615.
[27] R. People and J. C. Bean: Appl. Phys. Lett., 47, (1985) 322.
[28] J. Zhu, X. H. Wei, Y. Zhang and Y. R. Li: J. Appl. Phys., 100, (2006) 104106.
[29] H. C. Longuet-Higgins and M. D. V. Roberts: Proc. R. Soc. London, Ser. A, 224, (1954) 336.
[30] B. Lee and L. -W. Wang: Appl. Phys. Lett., 87, (2005) 262509.
[31] R. Fujii, Y. Gotoh, M. Y. Liao, H. Tsuji and J. Ishikawa: Vacuum, 80, (2006) 832.
[32] N. A. Surplice and R. J. D'Arcy: J. Phys. E, 3, (1970) 477.

(Received: July 9, 2009, Accepted: November 25, 2009)